

A Method for Modeling and Control Complex Tendon Transmissions in Haptic Interfaces

Simone Marcheschi, Antonio Frisoli, Carlo Alberto Avizzano, and Massimo Bergamasco

Simultaneous Presence, Telepresence and Virtual Presence - PERCRO

Scuola Superiore S. Anna - Pisa

a.frisoli@sssup.it

Abstract—One of the principal guidelines in the design of haptic devices is to provide a suitable mechanical design that can improve control performance and the force-feedback fidelity. Unfortunately these guidelines may conflict with other design objectives (reflected mass, balancing, dexterity) as well as with specifications given by users and applications. For haptic interfaces based on tendon driven actuation it is highly important to achieve an accurate model of friction losses in the transmission system, in order to be able to compensate for them through an active control.

In this paper it is reported a method for modeling and control complex tendon transmissions used for driving haptic devices and robots. The presented approach can operate in realtime with very low complexity; it is applicable to all kinds of serial manipulators and provides enough flexibility to allow identification of parameters and modeling of distributed friction phenomena all along the transmission. The approach has been implemented and tested on a 4 DOF exoskeleton system, the PERCRO L-EXOS.

I. INTRODUCTION

Tradeoffs in the design process are not always a pure matter of performance, as more and more frequently, when the quality of technology improves, ergonomic and functionality factors drive the design process. In applications which employ exoskeletons as HIs [9] [11] the design complexity is extremely high with respect to other HI-based solutions. Complex kinematic transmission designs are also used in medical applications [2], where the “minimal invasivity” issue dominates all over the other performance specifications.

Complex transmission designs often imply a series of drawbacks. While they allow to locate the motors far apart from the actuated joints, reducing the reflected mass and inertia, they introduce drawback effects such as coupling of joints, complex friction modeling and elasticity of the mechanics [3] [4] [1] [10]. For haptic interfaces based on tendon driven actuation it is highly important to achieve an accurate model of friction losses in the transmission system, in order to be able to compensate for them through an active control.

Conversely, the classical approach to transmission modeling assumes that transmissions can be modeled as a pure linear kinematic relationship mapping motor positions/torques to joint ones [7]. This model results to be inadequate when the complexity of the transmission increases and high fidelity is required in the replication of forces. Prisco in [6] analyzed the case of the control of a 3DOF system to achieve high performance, while Frisoli in

[5] considered the dynamic modeling of a transmission as an actuating mean for a parallel manipulator. The PERCRO L-EXOS shown in Figure 1 represents a typical example of a tendon actuated robotic system.



Fig. 1. The PERCRO L-EXOS exoskeleton.

This paper introduces a systematic approach to physically modeling a cable transmission in order to build a mathematical model that takes into account also friction losses and effect of coupling between joints. The approach followed allows to iteratively determine the force/torque contributions of the transmission at each joint and viceversa, in the same way as it is carried out with an Eulero algorithm in manipulator dynamics. The developed results developed have been applied for modeling the transmission system of the L-Exos. An innovative algorithm is proposed for computing the contribution of friction losses due to the cable transmission system, in case of coupling of joints, even if no force sensing measures are available on the system. The following sections will introduce the general theoretical formulation, the basic strategies for modeling and identifying the transmission parameters and the relative integration with a control system. The theory is also applied to a case-study: the PERCRO Light Exoskeleton (L-EXOS), an arm exoskeleton with 4 DOF for the force feedback on the upper arm. The complexity of the transmission makes this system particularly suitable for the application of the proposed method.

II. MODEL OF THE TRANSMISSION SYSTEM

We will limit our analysis to tendon actuated robotic systems which fulfill the following requirements:

- The structure of the system can be schematized as a serial kinematic chain composed of rigid links, linked by rotational joints;
- The transmission system is implemented with cables which start from actuators, are routed over a number of idle pulleys and reach the driven joints;
- The joint torques are transmitted with negligible deformation of structural mechanical parts; this hypothesis allows to ignore all local dynamic effects and to consider inertia contributions as an equivalent global inertia applied on motors or joint shafts.

A simplified scheme of such a kinematic structure is represented in Fig. 2. This constructive solution is frequently adopted when motors are placed far from the joints to be actuated. Nevertheless, this approach can be generalized to other constructive solutions. A speed-reducer may be present either on the first or on the last joint of the transmission.

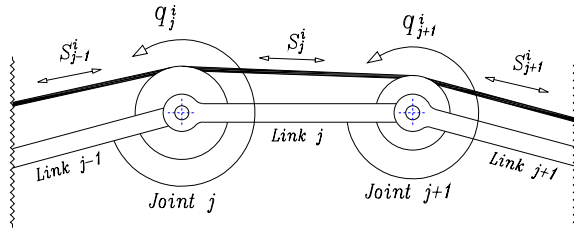


Fig. 2. Scheme of a particular transmission system

A. Kinematics of a tendon actuated mechanism

Considering a cable of the transmission i , which links the motor i to the correspondent joint i by crossing $i - 1$ intermediate joints, the following variables can be defined:

- r_j^i the radius of idle pulley placed on joint j and belonging to the transmission i ; r_i^i indicates the radius r_i^i of the last pulley of transmission i on joint i ;
- q_j^i the angular position of the idle pulley placed on joint j , evaluated with respect to the position of the previous link j ;
- S_j^i the displacement of the branch of the cable between joint j and $j + 1$, that belongs to the link j ;

Note that r_j^i is assumed with proper sign defined according to the cable routing (according to whether the routing is coincident or not with the sign convention adopted for the joint angle.). Pulleys with parameters characterized by $i \neq j$ represent idle pulleys (which allow the cable to cross the joint), while the ones characterized by $i = j$ represent driven pulley (which are fixed to the actuated link i and can produce its movement with respect to link $i - 1$).

The displacement of the branch of cable S_0^i of transmission i is determined by the rotation of the motor pulley q_m^i , which has a radius r_m^i , according to the following:

$$S_0^i = q_m^i r_m^i \quad (1)$$

Once the displacement S_{j-1}^i is known, it is possible to evaluate the angular position of the joint j and the displacement S_j^i by:

$$q_j = \frac{S_{j-1}^i}{r_g^i} \quad S_j^i = S_{j-1}^i - q_j r_j^i \quad (2)$$

where r_j^i is the generalized pulley radius¹.

As shown in Fig. 3 for a 3 DOF device, starting from motor positions, it is possible to calculate the actual positions of all the branches of the cable transmission by (1) and (2).

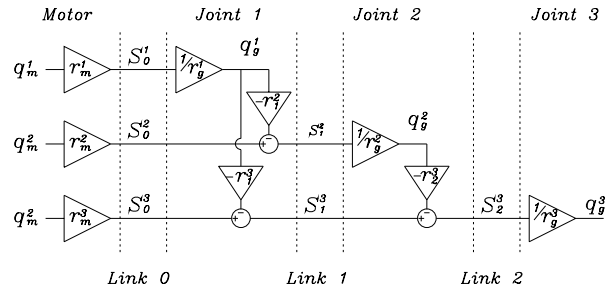


Fig. 3. Transmission Direct Kinematics

B. Statics of the transmission system

The following variables can be defined to describe the loads acting on the joint j :

- C_j^E the "external" torque resulting from the application of an external load on the end-effector; it can be evaluated by solving the static equilibrium for all the robotic structure, and resolving through the jacobian matrix the external force into torque joints;
- C_j^i the torque applied by transmission i on the joint j ; when $i \neq j$, this is the torque that is transmitted to the joint by a transmission crossing the joint, and that should be compensated by the other transmissions.
- C_m^i the torque applied by the motor connected to transmission i

Let τ_j^i be the tension of the cable of transmission i evaluated at joint j .

In the case of an ideal transmission, that is without loss of mechanical power along the cable routing, the cable tension remains constant along the routing and we have so:

$$\tau_1^i = \tau_2^i = \tau_3^i = \dots = \tau_i^i = \tau_i \quad (3)$$

¹It corresponds to the pulley radius, except in the case of a driven pulley ($i = j$) with an integrated speed-reducer: in such a case $r_i^i = r_{pulley} n_i$ where n_i is the transmission ratio of the speed-reducer.

With reference to joint j , once external torque C_j^E and all the tensions applied by the cables which cross the joint are known, the joint equilibrium equation allows to evaluate the tension on cable τ^j which acts on the joint j :

$$C_j^E = \sum_{k \geq j} \tau_k r_j^k \quad (4)$$

Equation (4) can be put in the form of a linear relation between the vector of the tensions induced by the external torques $\tau_j^E = C_j^E / r_j^j$ and the vector of the transmission tensions τ_j

$$\tau^E = K^T \tau \quad (5)$$

where K is the transmission matrix.

Supposing now that the transmissions are not ideal, reductions of cables tension will occur due to dissipative phenomena; it is necessary to introduce a new variable $\Delta\tau_j^i$ defined for transmission i as the difference between the cable tension between joint j and $j+1$ (reduction of tension in the part of transmission placed on link j):

$$\Delta\tau_j^i = \tau_j^i - \tau_{j+1}^i \quad (6)$$

In this case, the cable tensions which should be considered in (5) for the branch i depends also on the tension in the branch j .

We propose in this paper, a method to evaluate the tension of cables also in presence of dissipative losses of tension. As shown in Fig. 4, starting from the external torques, by (4) and (6) it is possible to evaluate the actual cable tensions for all the branches of the of transmission. This scheme can be easily numerically implemented, after that a proper identification of losses due to friction has been carried out.

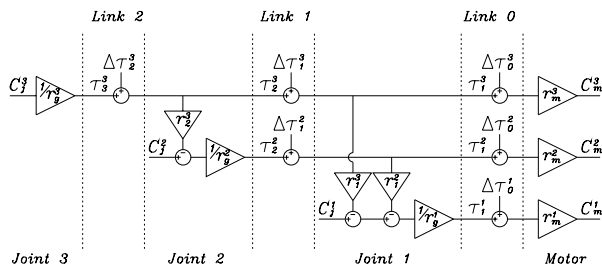


Fig. 4. The statics

C. Dissipative effects

The most important dissipative phenomena which affect cable transmissions are the following:

- friction on pulley supports;
- efficiency of cable transmissions;
- efficiency of speed-reducers if present.

A simple model for describing the torque friction M affecting radial ball bearings is the one proposed by the

constructors, that is described by the following relations:

$$M = \begin{cases} M_{ext} & \text{if } n = 0 \text{ and } M_{ext} < \alpha p \\ \beta p + h(n) & \text{if } n \neq 0 \end{cases} \quad (7)$$

where M_{ext} and p are respectively the external torque and the normal force acting on the bearing and n is its angular speed. Coefficients α and β depend on the bearing model and on the ratio between radial and axial components of the force p acting on the bearing, while function h has the following expression:

$$h(n) = \begin{cases} h_0 & \text{if } n < n_0 \\ h_1 n^{2/3} & \text{if } n \geq n_0 \end{cases} \quad (8)$$

where h_0 and h_1 are two constant depending on model of bearing, its middle diameter and type of lubricating (h_1 depends also on lubricating kinematic viscosity) and n_0 depends on lubricating kinematic viscosity.

The efficiency of cable transmission is related to following phenomena:

- elastic sliding between cable and driven pulley;
- internal friction between strands which compose the cable;
- friction induced by misalignment between cable and pulley.

The effect of reducer efficiency can be suitably described as follows:

$$M_{out} = \begin{cases} \eta_d \kappa M_{in} & \text{if } M_{out} n_{rid} \geq 0 \\ \frac{\kappa M_{in}}{\eta_i} & \text{if } M_{out} n_{rid} < 0 \end{cases} \quad (9)$$

where M_{in} and M_{out} are respectively the input and the output reducer torque, κ is the reducer ratio and η_d and η_i are respectively the direct and the inverse reducer efficiency. In the most common case that the dissipated power depends only on output power, and the relation between η_d and η_i is given by:

$$\eta_i = \frac{2\eta_d - 1}{\eta_d} \quad (10)$$

The presence of a speed-reducer with an high ratio can make the difference between η_d and η_i quite significative, becoming non negligible for the purpose of a proper compensation of friction.

III. PROCEDURES FOR IDENTIFICATION OF FRICTION PARAMETERS

All geometrical dimensions (i.e. pulley and cable radii) are supposed to be given with high precision (for example by 3D CAD models). The analytical characterization of all dissipative phenomena according to the model presented above, in general requires the evaluation of a very high number of parameters, which that can even modify their values over time. For this reason, a simplified model and an experimental approach based on the implementation of an automatic characterization procedure have been adopted.

The base operative hypotheses are the following:

- The efficiency of reducers and cable transmissions can be neglected with respect to the bearings friction; this is reasonable due to the high number of idle pulleys;
- Static friction phenomena are not characterized when they cannot be compensated; in fact, when device is provided only with motors position sensors and used as a force display, it is not possible to compensate them;
- As a first approximation, viscous friction can be expressed as a linear function of bearing speed, through a viscous friction coefficient ν ;
- All contributions due to the dynamic friction torques of all bearings of a given transmission and placed on a given link can be represented as a single equivalent torque (alternatively a single loss of cable tension); in fact, this group of bearings have the same speed rotation and are interested by forces which are all proportional to the same quantities ² (i.e. the speed and tension of cable): for this reason, the dependence of friction torque from speed and force is uninfluenced by the distribution over bearings.

According to the hypotheses made above, all dissipative phenomena can be represented as a loss in the cable tension which goes through a given link j as:

$$\Delta\tau_j^i = \beta_j^i \tau_j^i + \nu_j^i \dot{S}_j^i \quad (11)$$

where β_j^i and ν_j^i are the constants which express the linear dependence of the loss tension respectively with cable tension and cable speed.

A. Experimental procedure for identifying viscous friction

In a more simplified version of (11), the friction forces are considered independent of the cable tension τ_j^i :

$$\Delta\tau_j^i = \tau_{0,j}^i + \nu_j^i \dot{S}_j^i \quad (12)$$

A constant term is $\tau_{0,j}^i$ is added to consider the static friction due to the tension of the transmission.

The identification procedure for the acquisition of parameters of (12) can be carried on by recording the motor current during the movement, at a given speed, of the transmission to be characterized. The movement is obtained through a speed control scheme at constant velocity, to exclude the effect of inertial forces. For any transmission system, the motor torque C_m^i due to friction in transmission i , is assumed to be determined by the law:

$$C_m^i = C_{m,0}^i + \nu^i \dot{q}_m^i \quad (13)$$

For each transmission the unknown friction parameters ν^i and $C_{m,0}^i$ can be experimentally identified. The identification can be conducted according to two different strategies:

- S1. all remaining motors, but i , are controlled at zero speed;
- S2. all remaining joints, but i , are controlled at zero speed.

²This assumption is true in ideal conditions of inextensible cables and of negligible losses of cable tension due to the single friction torques.

In the condition S1, when the transmission j , to be identified, is moved, the branches of the other transmissions starting from motors up to joint j do not move; as it can be seen from the scheme in Figure 3, the joint speed \dot{q}_g^i is zero only for $i < j$, while for $i \geq j$ we have:

$$\dot{q}_i = - \sum_{k=j}^i \frac{r_k^i}{r_i^i} \dot{q}_j \quad (14)$$

This kinematic condition can be obtained only if the torque applied by the motor j is equal to the global friction torque of transmission j and also provides the friction contribution to move the parts of the transmission from joint j to EE. It should be considered that in this identification schemes both Coriolis and centrifugal apparent forces are generated during the motion of the links after joint j , and will affect the measure of friction force, when velocities become relevant.

In the condition S2, when the transmission j is moved, the others transmission branches are fixed with respect to the link only in the parts from joint j to the EE. Any motor which acts on a joint $i > j$ should allow the movement of the cable induced by rotation of the joint j : by measuring the correspondent motor torque it is possible to evaluate the friction torque relative to the part of the transmission from the motor up to the joint j . The measured torque for joint j corresponds to to the friction of transmission j , supposed that torques left by other transmissions which cross joint j are zero. However the condition of zero joint speed does not involve necessarily that these torques are zero: in fact, due to static friction, the cable branch, even if motionless, can still have a non null tension.

In conclusion, in both the two identification schemes, the evaluation of the global viscous friction of the transmission, through the experimental measure of C_m^i , is affected by an error depending on the residual friction in the branches after the actuated joint. By using (12), the maximum error in the evaluation of the friction term C_m^i , respectively in the case of conditions S1 and S2, can be expressed as:

$$\begin{cases} \text{S1: } C_{m,err}^i = \sum_{k=j}^n (\sum_{l=k}^l \tau_{0,l}^k + \nu_l^k \dot{S}_l^k) r_m^k \\ \text{S2: } C_{m,err}^i \leq \sum_{k=j}^n (\sum_{l=k}^l \tau_{0,l}^k) r_m^k \end{cases} \quad (15)$$

So the identification scheme S2 can be considered more reliable than S1, because the estimated residual error $C_{m,err}^i$ is lower and no apparent inertial forces (Coriolis and centrifugal) are generated by the movement of the links, because all the joints are blocked and no motion of the robot arm is induced.

We can put the relationship represented graphically in Figure 3 in an analytical form that is valid for conditions S1 and S2, by introducing for each transmission the kinematic coefficients k_j^i , that relates the branches velocities \dot{S}_j^i to the motor pulley angular velocity \dot{q}_m^i :

$$\dot{S}_j^i = k_j^i \dot{q}_m^i \quad (16)$$

Then by making an energetic balance of losses for each transmission i , the following condition should hold:

$$E_{loss,i} = C_{m,0}^i q_m^i + \nu^i q_m^{i,2} = \dot{q}_m^i \sum_j \tau_{0,j}^i k_j^{i'} + q_m^{i,2} \sum_j \nu_j^i k_j^{i'2} \quad (17)$$

that implies:

$$\nu^i = \sum_j \nu_j^i k_j^{i'2} \quad (18)$$

$$C_{m,0}^i = \sum_j \tau_{0,j}^i k_j^{i'} \quad (19)$$

(18) and (19) allow to compute the global value of ν^i and $C_{m,0}^i$ once the single components ν_j^i and $\tau_{0,j}^i$ are known. When sensors of the transmission tensions, are not available a predictive approach can be used to decompose the global terms over the single joints.

We devised an original method to compute an estimation of the terms ν_j^i and $\tau_{0,j}^i$, based on the experimental measure of ν^i and $C_{m,0}^i$. We can indicate for transmission i given weights for each joint as γ_j^i and α_j^i , such that an estimation of the unknown parameters is provided in the form $\hat{\nu}_j^i = \gamma_j^i \nu^i$ and $\hat{\tau}_{0,j}^i = \alpha_j^i C_{m,0}^i$. The constraints (18) and (19) should be verified by the estimates $\hat{\nu}_j^i$ and $\hat{\tau}_{0,j}^i$, that implies the following:

$$1 = \sum_j \gamma_j^i k_j^{i'2} = \sum_j p_j^i \quad (20)$$

$$1 = \sum_j \alpha_j^i k_j^{i'} = \sum_j p_j^{i'} \quad (21)$$

with $p_j^i = \gamma_j^i k_j^{i'2}$ and $p_j^{i'} = \alpha_j^i k_j^{i'}$.

In particular the values of p_j^i and $p_j^{i'}$ are the percentage losses of energy, due to friction forces, that are generated at each joint and represent the contributions that each joint of the transmission gives to the total loss. They can be estimated on the basis of the constructive realization of each joint of the transmission. Once an estimation of the losses is given in percentage, it is possible to compute the value of γ_j^i as $p_j^i = \gamma_j^i k_j^{i'2}$, since the parameters $k_j^{i'}$ are uniquely determined by the kinematics of the transmission. The same applies to α_j^i .

IV. EXPERIMENTAL CASE

The proposed model has been applied to a particular device, the Light-Exos³ exoskeleton, presented in [8] and shown in Fig. 1. It is a 4 DOF haptic interface, all actuated by a tendon transmission. The adopted solution of placing all motors on the first link required long cable transmissions with coupled joints. Each transmission of the exoskeleton is composed by a continuous steel cable which is fixed on the motor pulley and reaches the actuated joint after having routed over a number of idle pulleys, placed on previous joints. Each pulley is supported by radial ball bearings. In

³The system has been developed within "Museum of Pure Form" project in the 5th framework program of the EU. The IST and the European Union are acknowledged for their grants in sustaining the Pure-Form research.

joints 1, 2 and 4, a speed-epicycloidal reducer is integrated: tendon drives the pulley which integrate the pinion gear, while the three planetary gears are supported by a shaft which also makes the function of joint axis.

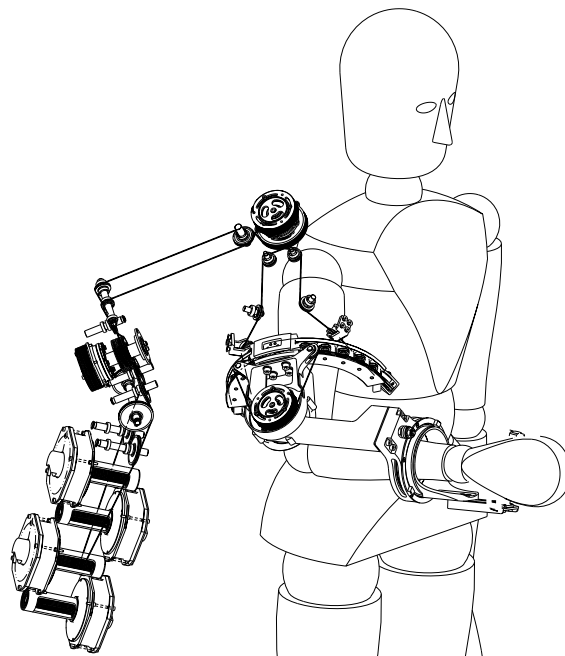


Fig. 5. The complex routing of transmission of L-Exos is shown for the 4th transmission.

The complexity of the transmission system is visible in Figure 5 where the transmission relative to the 4th degree of freedom is shown. The system can be schematized as a serial kinematic chain, composed by rigid links connected through rotational joints. For characterizing the dynamic behavior of the whole system, it is suitable to ideally separate mechanical components in the following subsystems:

- the structural parts,
- the transmission system, composed of tendons and pulleys.

A. Robotic structure

The *Direct kinematic* of the system is completely defined by the associated Denavit-Hartenberg parameters which allow to evaluate the homogenous transformation matrix between the different link frames.

In order to evaluate the velocity of the links, a formulation based on geometric Jacobian has been used. EE translation and rotation speeds are expressed by the following equation which describe the *differential kinematic* of the structure

$$\mathbf{v} = J\dot{\mathbf{q}} \quad (22)$$

where \mathbf{v} represents the generalized EE speed, \mathbf{q} is the vector of lagrangian variables, representing joint rotations and J is the geometric Jacobian matrix associated to the structure.

All the mass data (i.e. mass, geometry, centre of gravity and inertia tensors for all the links) and all geometrical dimensions have been estimated by 3D CAD models. The high precision manufacturing process, allows to conclude that most of data derived from the CAD design are reliable.

B. Control architecture

When the system is used for providing the force feedback, it is controlled to produce at the end-effector a desired value of force. The desired value of force is computed through the estimation of a desired position for the end effector, called \mathbf{X}_{god} , generated by a haptic rendering algorithm on the basis of the geometry simulated and the amount of penetration inside the object. The position of the end-effector $\hat{\mathbf{X}}$ is estimated through the Direct Kinematics law (DK block) from motor encoder readings (see Figure 6).

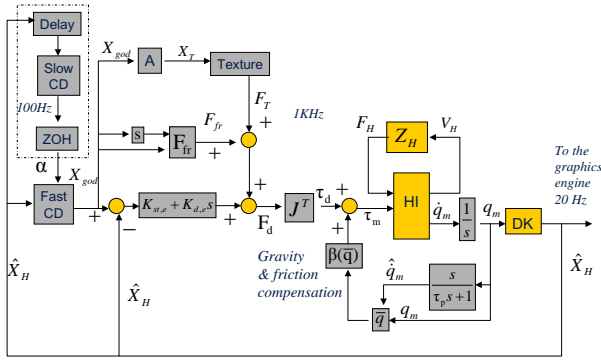


Fig. 6. The control scheme.

Additional terms are then added, \mathbf{F}_{fr} and \mathbf{F}_T to simulate surface properties of the object, based on local micro-geometry, such as friction and textures. Once that the desired value of force \mathbf{F}_d has been computed:

$$\mathbf{F}_d = (K_{st,e} + K_{d,e}s)(\mathbf{X}_{god} - \hat{\mathbf{X}}) + \mathbf{F}_{fr} + \mathbf{F}_T \quad (23)$$

a command torque is generated at motors to display this force at the end effector. A feedforward term $\beta(\bar{\mathbf{q}})$ is computed in order to compensate for friction and gravity errors. The computation of this feedforward term is based on an accurate model of the transmission system and of energy losses, according to the model presented in the previous section.

C. Experimental data

Figure 7 represents the equivalent torque applied at the first joint, during the manipulation in free motion of the end-effector in the two conditions of active (blue) or non (red) friction compensation. In the latter case the motors provide only the static torque necessary to achieve the gravity compensation. It can be noticed how the active compensation can reduce the effects of friction of more than 50%.

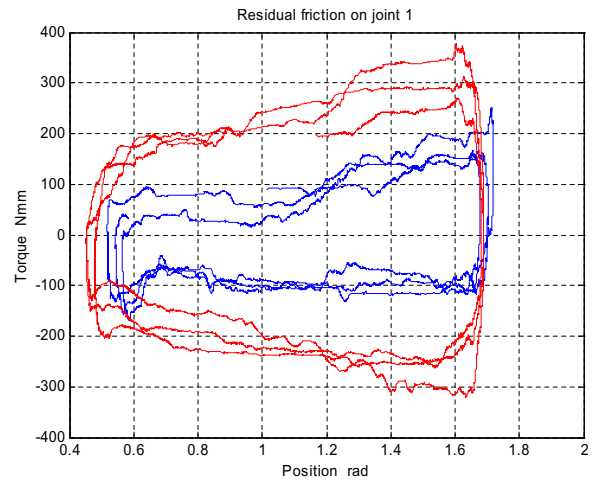


Fig. 7. Comparison of force required to move the exoskeleton at the EF with and without active friction compensation

V. CONCLUSIONS

This paper has presented a systematic methodology for modeling and identifying friction losses in tendon based transmission systems, valid also in case of coupled joints and availability of only position sensors. The identification scheme and the control strategy has been validated on the L-EXOS system, an arm exoskeleton with 4 dof for the upper arm, with good results. The control strategy for compensating friction of the transmission system can be applied when no force sensors are available along the structure, by using estimates of friction losses evaluated on the basis of the CAD model.

REFERENCES

- [1] Immersion corporation cybergrasp. <http://www.immersion.com>.
- [2] Intuitive surgical incorporation. <http://www.intuitivesurgical.com>.
- [3] F. Salsedo M. Bergamasco A. Frisoli, G.M. Prisco. A two degrees-of-freedom planar haptic interface with high kinematic isotropy. In *8th IEEE International Workshop on Robot and Human Interaction*, pages 297 – 302, 1999.
- [4] D. Mitropoulos E. Papadopoulos, K. Vlachos. Design of a 5-dof haptic simulator for urological operations. In *IEEE International Conference on Robotics and Automation*, volume 2, pages 2079 – 2084, 2002.
- [5] A. Frisoli. *Design and modeling of haptic interfaces: an integrated approach*. Phd thesis, Scuola Superiore Sant’Anna, Pisa, 2002.
- [6] M. Bergamasco G.M. Prisco. Dynamic modelling of a class of tendon driven manipulators. In *8th International Conference on Advanced Robotics*, pages 893 – 899, 1997.
- [7] B. Siciliano L. Sciavicco. *Modeling and control of industrial manipulators*. McGraw-Hill, 1995.
- [8] F. Barbagli M. Bergamasco, A. Frisoli. The museum of pure form. In *The 11th International Conference on Advanced Robotics*, 2003.
- [9] L. Bosio L. Ferretti G. Parrini G.M. Prisco F. Salesdo G. Sartini M. Bergamasco, B. Allotta. An arm exoskeleton system for teleoperation and virtual environments applications. In *IEEE Int.Conf.On Robotics and Automation*, pages 1449–1454, 1994.
- [10] P. Korondi H. Hashimoto N. Ando, P.T. Szemes. Friction compensation for 6dof cartesian coordinate haptic interface. In *IEEE/RSJ International Conference on Intelligent Robots and System*, volume 3, pages 2893 – 2898, 2002.
- [11] Woojin Chung Munsang Kim Chong-Won Lee Mignon Park Sooyong Lee, Jangwook Lee. A new exoskeleton-type masterarm with force reflection :controller and integration. In *IEEE Int. Conf. on Intelligent Robots and Systems*, volume 3, pages 1438 – 1443, 1999.